Anais da Academia Brasileira de Ciências (2019) 91(4): e20180165
(Annals of the Brazilian Academy of Sciences)
Printed version ISSN 0001-3765 / Online version ISSN 1678-2690
http://dx.doi.org/10.1590/0001-3765201920180165
www.scielo.br/aabc | www.fb.com/aabcjournal

Semi-automated counting model for arbuscular mycorrhizal fungi spores using the Circle Hough Transform and an artificial neural network

CLÊNIA A.O. DE MELO[1,2], JULIANE G. LOPES[2], ALEXSANDRA O. ANDRADE[2], ROQUE M.P. TRINDADE[2] and ROBSON S. MAGALHÃES[3]

[1]Universidade Federal da Bahia, Programa de Engenharia Industrial/PEI, Rua Aristides Novis, 2, Federação, 40210-630 Salvador, BA, Brazil
[2]Universidade Estadual do Sudoeste da Bahia, Departamento de Ciências Exatas e Tecnológicas/DCET, Estrada do Bem Querer, km 4, Universitário, 45083-900 Vitória da Conquista, BA, Brazil
[3]Universidade Federal do Sul da Bahia, Centro de Formação em Tecno-Ciências/CF-TCI, Rodovia de Acesso para Itabuna, Km 39, Ferradas, 45613-204 Itabuna, BA, Brazil

Manuscript received on February 18, 2018; accepted for publication on November 22, 2018

How to cite: MELO CAO, LOPES JG, ANDRADE AO, TRINDADE RMP AND MAGALHÃES RS. 2019. Semi-automated counting model for arbuscular mycorrhizal fungi spores using the Circle Hough Transform and an artificial neural network. An Acad Bras Cienc 91: e20180165. DOI 10.1590/0001-3765201920180165.

Abstract: Arbuscular Mycorrhizae (AM) are mutualistic associations between Arbuscular Mycorrhizal Fungi (AMF) and the roots of many plant species. AMF spores give rise to filaments that develop in the root system of plants and contribute to the absorption of water and some nutrients. This article introduces a semi-automated counting model of AMF spores in slide images based on Artificial Neural Network (ANN). The semi-automated counting of AMF spores facilitates and accelerates the tasks of researchers, who still do the AMF spore counting manually. We built a representative database of spore images, processing images through the Circle Hough Transform (CHT) method and training an ANN to classify patterns automatically. The classification analysis and the performances of the proposed method against the manual method are presented in this paper. The accuracy for the identification of spores by CHT in conjunction to ANN classification in the images was 90%. The results indicate that this method can accurately detect the presence of AMF spores in images as well as count them with a high level of confidence.

Key words: arbuscular mycorrhizal fungi spores, artificial neural network, circle Hough transform, image preprocessing, pattern classification, semi-automated counting.

INTRODUCTION

Arbuscular mycorrhizal fungi (AMF) colonize the roots of the majority of terrestrial plants (Smith and Read 1997). Mycorrhizal colonization is linked to the genotype of the plant and fungi, as well as the environment and diversity. According to Gianinazzi-Pearson (1996), the Arbuscular mycorrhizae (AM) association can be considered beneficial for both the plant and the fungus, in other words, it is a biological protection strategy.

The fact that many species interact with AMF shows the great importance of mycorrhizae for the preservation of flora and this stimulates increasing research on mycorrhizae (Smith and Read 1997). For instance, Tullio et al. (2012) showed that AM colonization was well established in pelargonium

Correspondence to: Clênia Andrade Oliveira de Melo
E-mail: clenia@uesb.edu.br
ORCid: https://orcid.org/0000-0003-3192-0283

plants on a horticultural substrate to satisfy the "sustainable floriculture" needs. Souchie et al. (2010) showed that among several P-solubilizing fungi isolates, the *Aspergillus niger*, PSF 7 and PSF 21 were the best isolates to increase clover (*Trifolium pratense*) growth in the presence of AMF.

The spores give rise to filaments called hyphae that develop in the root system of plants forming a tangle of hyphae, known as the mycelium. The mycelium contributes to the absorption of water and nutrients, especially phosphorus (Moreira and Siqueira 2006). Spores are reproductive structures of an asexual nature and they have a wide structural diversity (Goto and Maia 2006). These structures have varied characteristics, such as the number of layers and appearance, as well as color and wall thickness (Morton 1988). They measure from 22 to 1,050 μm (Schenck and Perez 1990, Schüßler et al. 1994).

It is important to count the spores because the greater the presence of AMF spores, the greater the positive effects that these fungi will have on plants, especially on species of economic interest (Siqueira et al. 1998, Moreira et al. 2015). Research shows that the presence of spores in soil can minimize the cost of agricultural inputs, such as mineral fertilizers, irrigation and pesticides, especially in the tropics where traditionally soils have low levels of phosphorus (Sieverding 1991). The application of a technology that promotes a reduction in the use of inputs can ensure efficient agriculture with environmental responsibility.

According to Walker and Vestberg (1998), in soil analysis, the presence and the quantity of AMF spores in a certain area can be determined, and manual counting is done by observing the samples through a microscope. Many minerals and organic particles that are present in these samples can lead specialists to make mistakes during the counting process. The sequence of tasks performed from the collection of the samples for the extraction of the spores to the manual counting of them can take hours. It is a task that requires expertise, attention and time.

Several studies related to AMF have been performed after the extraction and counting of AMF spores, including some with replicates of these processes at different times in the same work. Results from different collection points or comparing the counts in different seasons are some examples (Colozzi Filho and Cardoso 2000, Da Silva et al. 2015, Balota et al. 2011, Longo et al. 2014).

Technologies that use images to identify and to quantify microscopic objects can be effective tools as the automation of the counting process can improve working conditions and the results obtained by professionals who perform this activity (Groover 2007). Many researchers have studied automated methods to identify and to count objects contained in digital images. Using clustering, thresholding and segmentation, Melo et al. (2015) determined the number of somatic cells in cow's milk in microscope slide images for the detection of mastitis. The study by Kothari et al. (2009) was used for cell groups of four different cancerous tissues in digital images. Changyi et al. (2015) used Artificial Neural Network (ANN) and Circle Hough Transform (CHT) to detect and count apples from apple tree images taken in the field. Poomcokrak and Neatpisarnvanit (2008) and Nazlibilek et al. (2014) used ANN to classify and to count blood cells in digital images.

Some papers commonly apply ANN as an alternative classifier. Tan et al. (2014) used ANN to identify heterogeneous soybean seeds with several diseases. Zhaoyong et al. (2016) used a method based on transmittance spectroscopy and two classifiers (Support Vector Machine SVM and ANN) to detect moldy core in apples and types of symptoms. Ferreira and Galo (2013) developed a method of spatial inference of *chlorophyll a* concentration using ANN.

An algorithm that uses Gödel's fuzzy morphology operators was developed by Andrade

et al. (2015) to count AMF spores in a digital image, however, they used manually processed images, containing only spores (INVAM 2015).

This work proposes the semi-automated counting of AMF spores in a digital image to mitigate human error and the tedious nature of this task. In our research, the use of CHT in the preprocessing of the images to locate likely spores was tested. The database generated is the important contribution of this work. Another contribution is the incremental training. We adopted a hybrid method between an online method and a conventional ANN based-model for pattern classification, where we waived the use of the validation set.

MATERIALS AND METHODS

In this section, we describe the experimental setup and details of the proposed system called SDIC (System for Detection, Identification and Counting). Our algorithm relies on shape information to obtain sub-images of AMF spores and similar elements to them. We chose to apply the Circular Hough Transform (CHT) because it is based on the circular shape feature. The system uses CHT to find the patterns to be processed to compose the database. The patterns of possible spores located by CHT in the original image are cut into sub-images and some of the sub-images are resized by standardizing the data that will feed the ANN. The ANN algorithm relies on combining shape and color information in an MLP network for pattern classification. The details of all the steps are explained in the following subsections.

SAMPLE PREPARATION AND MANUAL COUNTING METHOD

The manual counting method starts with the extraction of AMF spores present in soil sample of a certain volume (Morton 1988). The expert can extract the spores using the Wet Sieving Process (WSP) proposed by Gerdemann and Nicolson (1963), followed by centrifugation in water and sucrose. The WSP is a long process and can be checked in INVAM (2015). This is also the basic process of spore extraction established in the Soil Microbiology Laboratory at the UESB (Universidade Estadual do Sudoeteste da Bahia), Vitória da Conquista, Brazil. For this study, the soil samples were collected from the UESB field.

The expert identifies and counts the spores with the help of a microscope alone putting the material in a Petri dish on top of graph paper that serves as a guide. The Petri dish is carefully moved and the number of spores that have been identified by observation are recorded manually (INVAM 2015).

THE SDIC SYSTEM

This subsection describes the setup used in the experiment from the acquisition of the images. The SDIC comprises a glass Petri dish, a microscope (S8AP0 model, Leica Microsystems), a camera (DFC 295 model, attached to the microscope) and a Desktop Computer (Intel Core ™ i5-3330 CPU @ 3.00 GHz, RAM 4.00 GB, operating system Windows 7 Ultimate, Software: LAS V4.3). The acquisition of the images was performed at the Biological Control Laboratory at UESB. We decided to implement the algorithm in MATLAB® software (Trauth 2006) because of its collection of libraries of specific functions for Computational Vision and ANNs. We used the Remote Access Server (QEMU Virtual CPU version 2.39 GHz, 8 processors, RAM 4.00 GB, operating system Windows Server 2008 R2 Enterprise), belonging to UFBA (Universidade Federal da Bahia).

The preprocessing steps and ANN classification are automated phases. Spore extraction, image acquisition, and identification and classification by the expert are the manual steps of the system.

THE ACQUISITION OF THE IMAGES

The expert checks the spores in a microscope and uses a camera attached to the microscope to

record digital images. The images are obtained considering:

- The Petri dish is on graph paper. The images record only the areas containing spores. There are no repetitions in the areas of record already captured.
- There is an optical magnification of the image at 40x. This image magnification is enough for the expert to distinguish the spores from the other objects that appear in the image.
- There is an appropriate lighting system. This ensures a better display of spores.
- These original photos (2,048 x 1,536) pixels are saved the in JPEG format, in a database.

IMAGE PREPROCESSING (DATABASE ORGANIZATION)

Recognizing objects in a two-dimensional image can be described as a sequence of actions to find and label the parts of a scene contained in that image. The characteristics and standards of each object to be recognized must be established. These patterns must contain object-specific information, such as shape, texture, and color (Acharya and Ray 2005).

To here spores that are part of the ANN database were identified from external appearance, discarding the discrepant characteristics and considering those with uniform coloration, with shades of yellow to dark brown and most of the spores analyzed in the region were globular in shape.

An image containing the objects to be identified must be preprocessed (segmented) through an edge detection filter and a binarization filter. The segmented images must be processed using a shape recognition technique and it is here that it is possible to apply the Circle Hough Transform (CHT). CHT is an efficient tool for recognizing and locating circular shapes in an image (Duda and Hart 1972). This processing is the step that identifies and locates the geometric shapes compatible with the spores of AMF. By using CHT it is possible to detect a curve in an image, even if the curve is barely visible or belongs to a noisy image.

A curve contained in a digital image, if it can be represented by its parametric equation, can be detected through CHT (Tsuji and Matsumoto 1978, Atiquzzaman 1999, Chen and Chung 2001). In the detection of circles, the equation of the circumference in its parametric form can be used (Eq. 1):

$$\begin{cases} x = a + R \cdot cos(\theta) \\ y = b + R \cdot sin(\theta) \end{cases}, \qquad \text{(Eq. 1):}$$

where (a,b) are the coordinates of the center of the circle, R is the radius of the circle and the variable θ is the angle between and the horizontal axis (θ is the common parameter).

Detecting circles in images through CHT uses the voting process. The operation of CHT occurs through a three-dimensional accumulator matrix (Atherton and Kerbyson 1999), which must find the value of its radius (R) or at least has a given value interval. The pixels contained in the edge segmented binary image are recognized as candidate pixels at the edges of a real circle. A candidate pixel casts the votes in the array of accumulators in a pattern around it, forming a full circle with a fixed radius. The votes of candidate pixels belonging to a real circle tend to accumulate at a point in the array of accumulators corresponding to the center of the circle. Therefore, the center of a circle is estimated by detecting the largest vote in the array of accumulators (Barber et al. 2001).

When the CHT algorithm is applied, it finds the centers corresponding to the edges of the circular elements of radius belonging to the stipulated interval (Yao and Yi 2016). In this study, the CHT is used to find the (a,b) locations of the circles throughout the image given a range of R corresponding to the minimum and maximum radius of the likely AMF spores. The algorithm used within MATLAB® to achieve this is based on the

accumulator array computation, center estimation and radius estimation (Djekoune et al. 2017).

Among the objects recorded in the images, besides the spores, other materials such as hypha fragments are often present in the collected soil samples (Figure 1a). However, the CHT selected set does not contain elements with non-circular shapes (Figure 1b).

CHT did not fail to detect any curves that are spores, even those with irregular shapes. However, it also detected some curves in the material which not spores. Therefore, it is necessary to separate occurrences in each class. A technique to do this is the use of an ANN as classifier, because once trained, the ANN can generalize the information to an unknown set of examples, emulating the human brain.

After CHT locates the circular elements, we return to the RGB (Red, Green, Blue color space) images and classify each sub-image by ANN. RGB color space was created to represent digital images in order to specify colors in a given pattern. These digital images are represented as arrays of color components of red, green and blue. The intensity of the red, green and blue components is represented with integer values from 0 to 255, representing the pixels in this space (Gonzalez and Woods 2010).

INPUT DATA

Preprocessing was applied to the images using some MATLAB® functions, in an empirical way. The application of these functions provided patterns in the appropriate format for ANN inputs. The procedure is described below.

- Create a copy of the original image in binary form. These binary images were used only for the location of possible spores by CHT and scaling of the sub-images.
- Apply CHT to the negative binary images, locating objects belonging to a radius of a predetermined interval. Initially we obtained binary images with white background and black elements.
- Crop the object detected by CHT in the original image getting the smallest window around this object (Figures 2a and 2b). Each window around an object located by CHT, in the original images (2,048 x 1,536) pixels, generates other small images with sizes between (42 x 42) and (114 x 114) pixels. With this, we can process the entire image through a finite amount of sub-images in a finite amount of time. A similar procedure was applied by Nazlibilek et al. (2014).

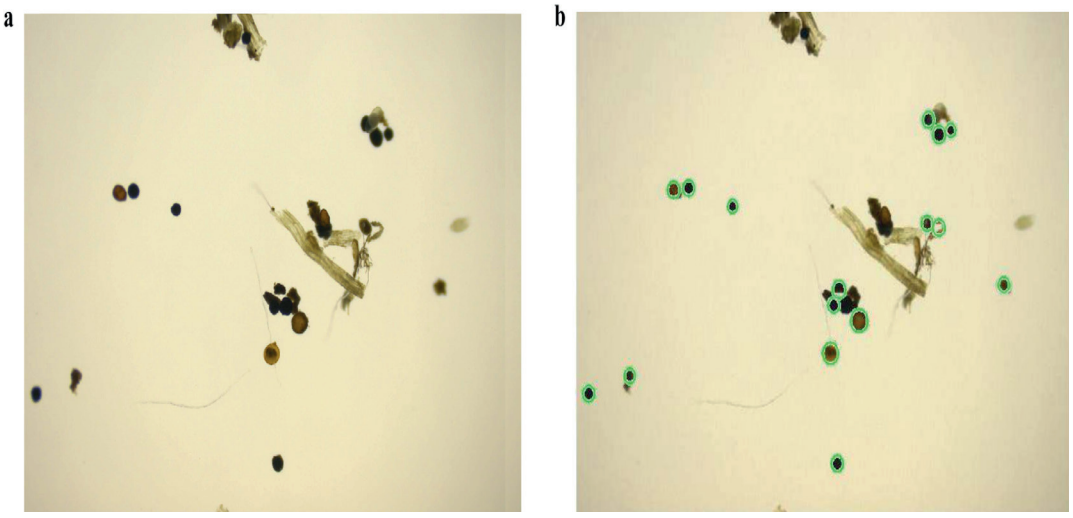

Figure 1 - Original Image **(a)**; Patterns found by CHT in original image **(b)**.

- Resize all the sub-images generated to a standard size (Figure 2c). The default size is defined as the size of the sub-image containing the smallest spore shape. Each sub-image was resized to the size 42 x 42 pixels. The great advantage of resizing the sub-images is to standardize all data with a smaller number of ANN input signals. There was no analysis of information loss from the images that were resized as 100% accuracy was achieved in learning the patterns during the training. After these steps, the binary images are discarded and we return to work with RGB images.
- Obtain RGB arrays in a vector form and compose the sub-images. The resulting vectors from each sub-image are concatenated, forming an array that contains all the objects detected by the CHT in the image.
- Save the arrays in a digital document.
- All patterns presented to the ANN, which compose the training set and the test set, are comprised of input vectors (Eq. 2) with a constant length *n*.

$$\{x_i\}_{i=1}^{n} \quad \text{(Eq. 2)}$$

The equation (Eq. 3) gives the length (n) of each input vector.

$$n = (l \times c) \cdot q \quad \text{(Eq. 3)}$$

where $(l \times c)$ are the dimensions of the sub-image and is the number of necessary arrays for the composition of colors.

The input patterns to ANN are sub-images found by the CHT technique, resized and converted to vector form. After this, an AMF expert classifies the patterns as 'spores' or 'non spores' by visual observation.

EXPECTED OUTPUTS

Before the application of ANN, it was necessary to establish the data sets with the corresponding inputs and expected outputs (targets), because we chose a supervised learning rule. The supervised learning rule requires the comparison between the ANN output and the target. Thus, for each input presented to ANN, this ANN produces an output.

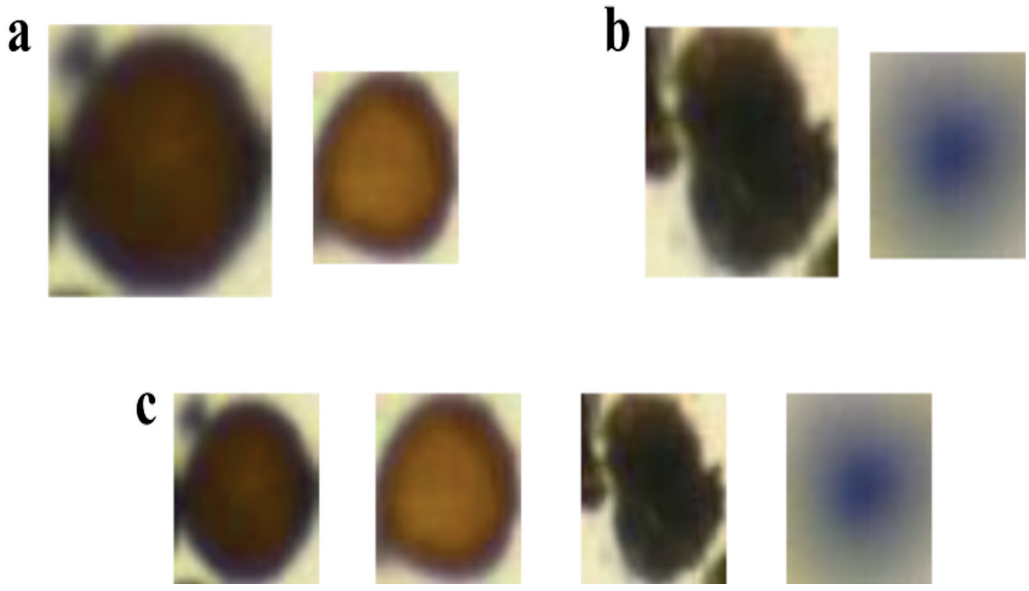

Figure 2 - Patterns found by CHT in RGB sub-images: 'spore' pattern in RGB sub-image (**a**); "non spore" pattern in RGB sub-image (**b**); The RGB sub-images resized (**c**).

This output is compared with the target, and the algorithm adjusts the synaptic weights, until the ANN answer (output) is increasingly close to the target (Haykin 1999).

In the formation of the output vector, the targets were generated from each input pattern (sub image vector) detected by the CHT. The classification between 'spore' and 'non spore' is made as a preliminary assessment from an AMF specialist. Therefore, it was recorded that:

- input pattern (sub-image vector) containing a 'spore' is given as a desired count or "target 1";
- input pattern (sub-image vector) containing a 'non spore' is given as a non-desired count or "target 0".

The application of this rule comprises the output vector. After training, the ANN should be able to classify these patterns.

ANN MODEL STRUCTURE

ANNs deal mainly with function approximation problems, data clustering and pattern classification (Basheer and Hajmeer 2000) while MLP networks are those containing more than one layer with one or more neurons in each layer (Haykin 1999).

The ANN structure used in this study is a multilayer perceptron (MLP), feedforward, with one hidden layer, and the tangent sigmoid function in the activation function (Figure 3).

An important component of training is to establish an ending criterion for the learning algorithm. We defined the network-training stop as the mean square error (MSE) reduced to a sufficiently low rate according to a predetermined parameter during the training phase.

The training phase ends the process when the mean square error (MSE) reaches a minimum value. For each training set, the MSE obtained the minimum value in different epoch quantities. The average number was 7 epochs. The network was able to learn 100% of the training examples, stopping training when the error converged to zero.

The computational cost of the training is polynomial as a function of the number of epochs. The computational cost of the algorithms of test and validation is linear due to the parallelism of ANNs (Haykin 1999). Models based on ANN after the training phase have the advantage of optimizing the time and computational effort to find the solution (Fang et al. 2004). The average time spent was 87 seconds during the training and 0.42 seconds during the test.

We used a hybrid method of training between the online method and the traditional method, where we did incremental training. The data were divided into 22 (twenty - two) training set - test set pairs; each image acted both as a part of a training set and as an independent test set. The training set was used for neural network learning; the test set was used to estimate the performance of the neural network on the data set that was not trained during learning. We did not use a validation set. A similar method can be found in Su et al. (2014). The experiment followed these steps:

- There was training with 807 patterns (S1 set).
- Then each image of the test set was sequentially presented to the network. The test sets have untrained patterns.
- The results obtained by the network were recorded (by image).
- As the new patterns (by Image) are presented to the networks, and the network output is evaluated, the new patterns are immediately incorporated into the training set.
- New network training is carried out. The network learns from patterns that were not initially contained in the training set. The new set was trained using the initial weight matrix that resulted from the previous training.

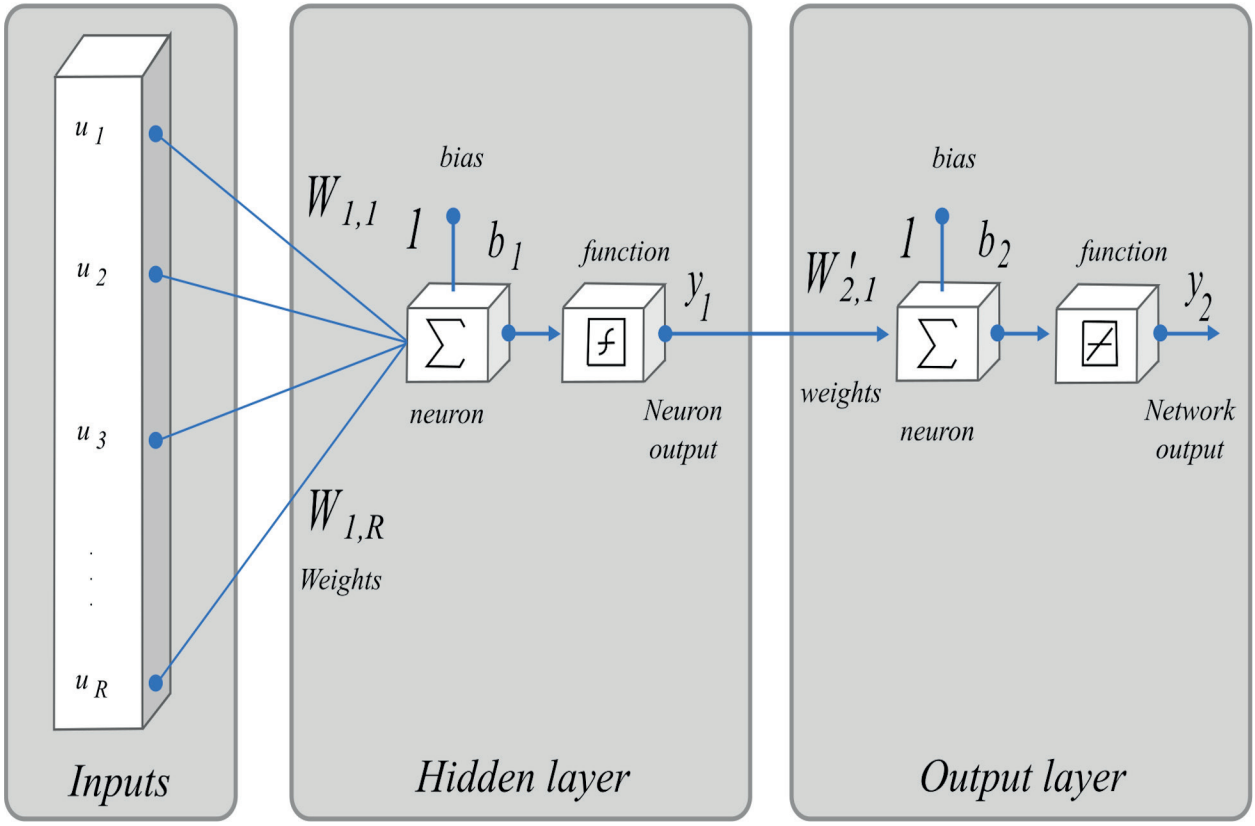

Figure 3 - Feedforward ANN structure.

- This sequence continues until we use all training-test data set pairs.
- We tested 22 sets (images). These test sets had a number of patterns ranging from 6 to 77 elements.

The successful test of an ANN occurs when it correctly classifies the new patterns presented, i.e. when there is good generalization during the test of the ANN (Freeman and Skapura 1991).

With an MLP network structure composed of a minimum amount of neurons, it obtained very good generalization and was able to improve the results of the work proposed by Melo et al. (2017) to count the AMF spores using an elemental ANN, the Perceptron. The accuracy in the classification of their test set was 77% and 1,108 patterns were selected and incremental training was not used. Therefore, besides the amount of data being different, the method of training was also different. The work of Melo et al. (2017) separated one set for training (73% data) and one set for testing (27% data).

THE FUZZY MORPHOLOGY METHOD

In this section, we present published work. The fuzzy morphology method uses fuzzy logic, more specifically, Gödel's erosion, in the spore counting of mycorrhizal fungi in clean images (Andrade et al. 2015). In this method another image is used, called the structural element, to change the original image.

The method is composed of four steps: 1) Apply Gödel's erosion. 2) Use binary image. 3) Apply a mask that removes small connections between spores. 4) Count the spores using the average (Gonzalez and Woods 2010). This method was applied to the 22 pre-processed images with CHT and we compared the test results with our method. We call this the CHTFM method. Initially, the background color was changed to black due

to the use of the fuzzy erosion operator. Then the images were resized to (1,000 x 750) pixels and finally processed.

STATISTICAL ANALYSIS

With a statistical analysis, we can identify which AMF spore counting method is able to replace the manual counting of these spores more efficiently in the circumstances presented in this research. For this task, we chose the Bland-Altman method (Bland and Altman 1986), which evaluates the discrepancy between the two measures. We built the correlation chart and scatter plot that shows the mean of the measurements.

In this method, the correlation between the analyzed measures, bias, standard deviation and the limits of agreement was calculated. To determine the variables and graphics we used the free software R, comparing the SDIC method with the Manual method and the CHTFM method with the Manual method.

The Manual method established the classification and quantity of spores that were considered as reference for this study. The results of the classification obtained using the SDIC and the CHTFM methods were compared to the reference results established by the Manual method. The Kappa Test analyzed the agreement between the SDIC method and Manual method and analyzed the agreement between the CHTFM method and Manual method (Carletta 1996). We used the method proposed by Landis and Koch (1977) to interpret the value obtained by the Kappa Test.

RESULTS AND DISCUSSION

From the image repository, we selected 40 images that generated 1,282 patterns. A set with 18 images generated a training set with 807 patterns, and a set of 22 images generated a test set with 475 patterns. The training set has fewer images than the test set, but it has more input patterns because the number of structures in each image can vary widely.

EXPERIMENTAL RESULTS

The results of the ANN simulations can be found in Table I. The expert had previously observed all the images and counted the spores (Manual Spores Quantity). The average accuracy was 90% when compared to manual counting.

In the test set (475 patterns) of the 350 spores detected by the expert as “target 1”, the SDIC correctly classified 321 patterns as “target 1”, and 29 patterns as “target 0”, false negative ones (FN). There were 125 patterns “target 0” and the SDIC correctly classified 101 patterns as “target 0”, and 24 of them as “target 1”, false positive ones (FP). In the test phase, the SDIC incorrectly classified 53 patterns (FN + FP) of the 475 patterns.

Mineral and organic particles from the extraction process with a shape and color similar to those of the spores can be misclassified. This was a limitation encountered during the classification and counting of spores by ANNs. The edges of the circular Petri dish are not captured by the rectangular images of the camera, and the specialist is responsible for grouping the spores in the visible area of the Petri dish.

The rule supervised learning was used. Every time there was a difference between the output value provided by the ANN and the expected output value, the ANN adjusted the weights. The trained network achieved the classification error zero criterion, therefore the network learned 100% of the training examples. The ANN training phase was a match with the expert count (manual).

The acquired results in the test indicate that it is feasible to detect AMF spores in a digital image using the CHT technique. ANN is an effective tool for the classification of patterns from the generated database. The test results show that the SDIC has a good generalization ability.

TABLE I
Training sets and results of the Test sets for SDIC method.

Training (SDIC)								Test (SDIC)			
Set ID	Accumulated Patterns Quantity	Epochs	Time (s)	New Image ID	New Patterns Quantity	Manual Spores Quantity	CHTFM Spores Quantity	Spores Quantity	Time (s)	Error number (classification)	Hit (%)
S1	807	14	146	1	11	8	8	8	0.63	2	82
S2	818	1	27.2	2	19	19	18	16	0.83	3	84
S3	837	5	76.8	3	15	14	10	14	0.21	0	100
S4	852	2	45	4	21	14	15	13	0.2	1	95
S5	873	4	83	5	41	32	45	32	0.89	6	85
S6	914	5	93.1	6	40	28	31	28	0.9	4	90
S7	954	3	57.8	7	38	29	34	30	1.07	5	87
S8	992	10	112	8	16	9	15	7	0.56	2	88
S9	1008	34	306	9	18	13	18	13	0.25	0	100
S10	1026	1	22.7	10	14	13	14	13	0.55	0	100
S11	1040	1	24.7	11	11	9	11	10	0.41	1	91
S12	1051	4	75.3	12	10	10	11	10	0.45	0	100
S13	1061	0	3.7	13	9	8	7	8	0.37	0	100
S14	1070	1	24.1	14	6	2	5	2	0.19	0	100
S15	1076	1	23.3	15	22	19	24	17	0.24	2	91
S16	1098	2	30.8	16	21	16	23	14	0.23	4	81
S17	1119	10	118	17	77	54	73	55	0.4	11	86
S18	1196	20	207	18	12	10	9	8	0.2	2	83
S19	1208	17	176	19	19	8	22	10	0.3	2	89
S20	1227	6	43.2	20	21	16	18	16	0.24	2	90
S21	1248	5	153	21	19	9	19	10	0.06	3	84
S22	1267	6	75.8	22	15	10	13	11	0.11	3	80

The same test images, containing only the elements located by CHT, were processed and adjusted for a spore analysis and counting using the fuzzy morphology method proposed by Andrade et al. (2015). This was the nearest work found despite the fact that it focuses on counting separate spores in the images mechanically.

A database was created with the new images containing only the structures detected by the CHT technique and kept the coordinates of the detected structures in the binary images. In these new images, all structures that were not detected by the CHT were converted to white. The fuzzy morphology method (CHTFM) used the same processed images as the SDIC. The counting results obtained by this method were compared with the results of this study. The best results were obtained when the models proposed here were applied.

We compared the results of the methods in all of the 22 images used in the test phase. The manual method identified and counted 350 spores of the 475 patterns presented in the test set. The SDIC identified and counted 345 elements as spores. Regarding the manual method, SDIC obtained a deviation of 1% in spore counts. The CHTFM method identified and counted 443 elements,

obtaining a deviation of 27% in the number of spores counted using the manual method.

In the test set (475 patterns), of the 350 spores detected by the expert as "target 1", the CHTFM correctly classified 325 patterns as "target 1", and 25 patterns as "target 0", false negative ones (FN). There were 125 patterns "target 0" and the CHTFM correctly classified 7 patterns as "target 0", and 118 of them as "target 1", false positive ones (FP). In the test phase, the CHTFM incorrectly classified 143 patterns (FN + FP) of the 475 patterns. The CHTFM method did not detect any elements with dimensions less than 30% of the average of the dimensions of the standard elements and occasionally counted in duplicate elements with a dimension larger than the average of the dimensions of the standard elements.

The Kappa Test value for the agreement evaluation between the SDIC method and Manual method was $k \cong 0.70$. For the results presented using the SDIC method, the Kappa test (k) was framed in the category range "substantial agreement" when compared to the manual method.

The Kappa Test value for the agreement evaluation between the CHTFM method and Manual method was $k \cong 0$. For the results presented using the CHTFM method, the Kappa test (k) was framed in the category range "no agreement" when compared to the manual method.

Using the Bland-Altman method, we found the correlation and agreement of the SDIC with the manual method with the aid of the scatter plot and the correlation coefficient. We used the same method to verify the correlation and agreement of the CHTFM method with the Manual method. With this statistical study, we analyzed the counting result in the test sets.

A statistical analysis was performed comparing the SDIC method with the manual method and the CHTFM method with the manual method. The comparison between the SDIC method and that of CHTFM was only qualitative.

The MCM significantly affected the count values for the CHTFM (Table II) with $p < 0.001$.

The manual method and the CHTFM method were analyzed using manipulated images with CHT. These two methods showed a strong correlation because the correlation coefficient is $r = 0.95$ (Figure 4a). However, the Bland-Altman method graph showed low agreement between the CHTFM method and the manual method (Figure 4b). The measurements do not agree because the bias is statistically significant, and increases as the average between the measurements increases. There was a high correlation between the manual method and the CHTFM, but there was no agreement between them.

The MCM significantly affected the count values for the SDIC (Table III) with $p < 0.001$.

We analyzed the manual count of spores done by the expert and by the SDIC method count. These two methods showed a strong correlation with a correlation coefficient of $r = 0.99$ (Figure 4c). The Bland-Altman method chart revealed high agreement between the manual and SDIC methods (Figure 4d), because the bias is close to zero and the correlation threshold is small. The correlation threshold is close to 5. In addition to a high correlation between the manual method and the SDIC, there was also a "substantial agreement" between them.

According to this statistical study, we can conclude that the SDIC is a promising automated method that can replace manual counting in complex images containing spores and similar materials to them.

The proposed method was not limited to counting the elements that appear in the images, but it also classified these elements as 'spores' or 'non spores'. The statistical results between the classification of the data by the proposed method and the classification by the manual method reflect the consistency of these data obtained through the CHT and used to validate the model.

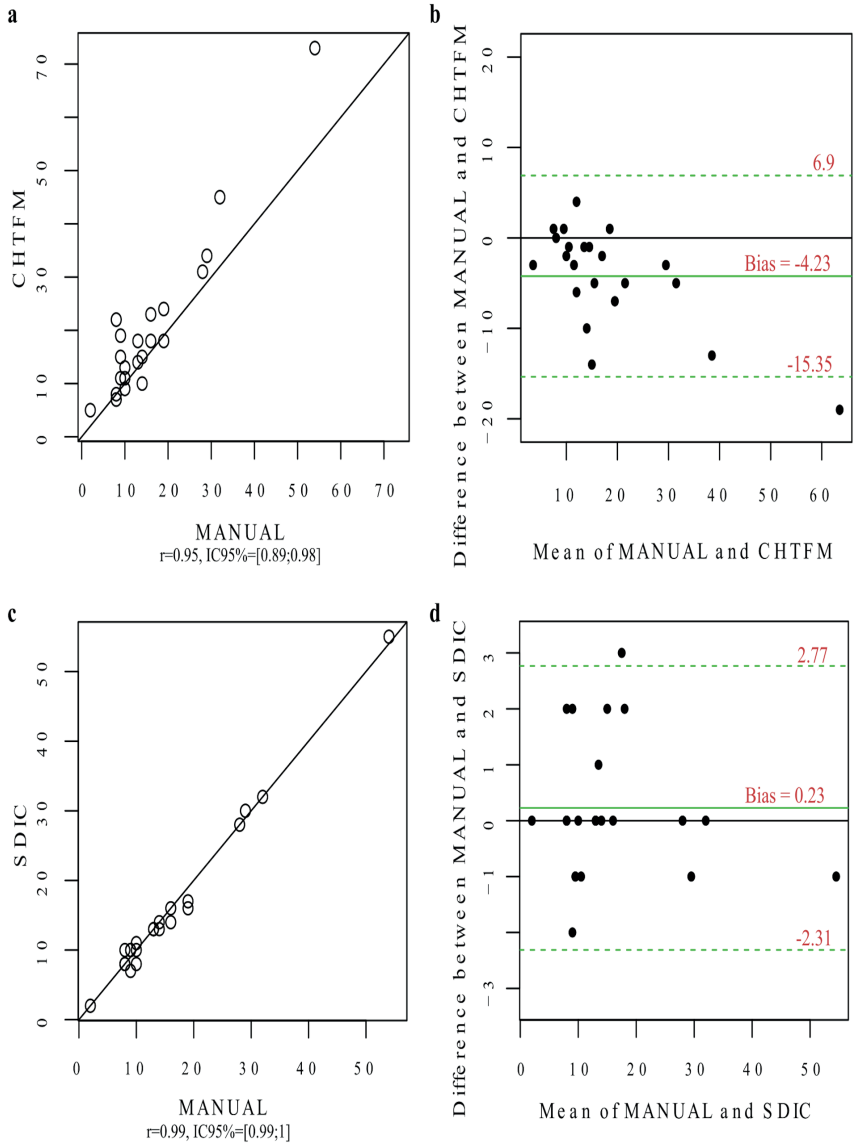

Figure 4 - Correlation graph between the Manual method and the CHTFM method **(a)**; Bland-Altman graph between the Manual method and the CHTFM method **(b)**; Correlation graph between the Manual method and the SDIC method **(c)**; Bland-Altman graph between the Manual method and the SDIC method **(d)**.

TABLE II
Analysis of the regression models of the MCM variable as a function of the CHTFM variable, performed in 22 test images (test sets).

CV	DF	Sum Sq	Mean Sq	F. Value	Pr (>F)
MCM	1	4406.8	4406.8	199.48	7.262*
Residuals	20	441.8	22.1		

*significance at 0.1% levels ($p < 0.001$).

TABLE III
Analysis of the regression models of the MCM variable as a function of the SDIC variable, performed in 22 test images (test sets).

CV	DF	Sum Sq	Mean Sq	F. Value	Pr (>F)
MCM	1	2755.19	2755.19	1640.8	2.2*
Residuals	20	33.58	1.68		

*significance at 0.1% levels ($p < 0.001$).

The contribution of our paper lies in the following aspects. We have successfully used ANN to count AMF spores in images and achieved better performance compared with a previously published work. Our generated individual data presentation using CHT provided the ANN classifier with an efficient way to classify the data.

CONCLUSIONS

Manual counting of AMF spores is a common task in soil microbiology laboratories. Given that it is a relevant task for the studies of AMFs, the SDIC model is proposed to perform automated counting of AMF spores. Based on an MLP, this model was shown to be efficient enough to replace the manual spore counting method.

The SDIC model overcame the difficulties of identifying the analyzed structures. These difficulties arise from the similarity between the spores and other structures recorded in the photos acquired in the experimental setup. The SDIC achieved 90% accuracy in the classification and counting of the spores present in the images tested. There was a strong correlation between the SDIC results and the manual counting method, therefore presenting a viable alternative.

The research contributed to the creation of a repository of 40 images from the soil samples, which underwent the process of spore extraction. The pre-processing of the images and the resizing of the sub-images extracted by the CHT are essential for the classification process performed by SDIC based on an ANN. The adjustment of this ANN occurred through an incremental training procedure. This procedure proved to be more efficient than the procedure with one set for training and one set for testing applied by Melo et al. (2017).

In future work we intend to develop a feature to decrease the amount of network input signals data and improve the performance of SDIC. Visual analysis and statistical analysis of the basic attributes of the AMF spores can be done and classification based on the data features can be made. Other future work could consider analyzing an ANN with only the output layer instead of an MLP network. With these results, we will be able to compare two ANN structures. Further research may also justify why these selected patterns provide good results in the experiments.

ACKNOWLEDGMENTS

The authors thank Professor Divino Levi Miguel for the extraction of the spores and technical support in identifying them. We are also grateful to our collaborator Alécio Santos Barros. We thank the Universidade Estadual do Sudoeste da Bahia (UESB) and the Graduate Program in Industrial Engineering at Universidade Federal da Bahia (UFBA), for the materials and equipment available for the development of the research.

AUTHOR CONTRIBUTIONS

Each author contributed individually and significantly for the development of the study. CAOM developed the theoretical framework and took the lead in writing the manuscript, CAOM and JGL contributed to sample preparation and made the simulations, CAOM, AOA, RMPT and RSM contributed to the interpretation of the results. RSM was involved in planning and supervised the work.

REFERENCES

ACHARYA T AND RAY AK. 2005. Image Processing: Principles and Applications 15(3): 454.

ANDRADE AO, TRINDADE RMP, NEVES VBF, BARROS AS, SOARES IB, COSTA RP, MIGUEL DL, SANTIAGO RHN AND GUERREIRO AMG. 2015. Analysis of Fuzzy Morphology in Spore Counts of Mycorrhizal Fungi. 2015 NAFIPS Held Jointly with 2015 5th WConSC. IEEE: 1-8.

ATHERTON TJ AND KERBYSON DJ. 1999. Size Invariant Circle Detection. Image Vis Comput 17: 795-803.

ATIQUZZAMAN M. 1999. Coarse-to-Fine Search Technique to Detect Circles in Images, Int J Adv Manuf Technol 15(2): 96-102.

BALOTA EL, MACHINESKI O AND STENZEL NMC. 2011. Response of acerola to arbuscular mycorrhizal fungi under different levels of phosphorus. Bragantia 70(1): 166-175.

BARBER P, VOJNOVIC B, KELLY J, MAYES CR, BOULTON P, WOODCOCK M AND JOINER MC. 2001. Automated counting of mammalian cell colonies. Phys Med Biol 46: 63-76.

BASHEER IA AND HAJMEER M. 2000. Artificial neural networks: Fundamentals, computing, design, and application. J Microbiol Methods 43(1): 3-31.

BLAND JM AND ALTMAN DG. 1986. Statistical methods for assessing agreement between two methods of clinical measurement. Lancet 1(8476): 307-310.

CARLETTA J. 1996. Assessing Agreement on Classification Tasks: The Kappa Statistic. Comput Linguist 22: 249-254.

CHANGYI X, LIHUA Z, MINZAN L, YUAN C AND CHUNYAN M. 2015. Apple detection from apple tree image based on BP neural network and Hough transform. Int J Agric Biol Eng 8(6): 46-53.

CHEN T AND CHUNG K. 2001. An Efficient Randomized Algorithm for Detecting Circles. Comput Vis Image Underst 83: 172-191.

COLOZZI FILHO A AND CARDOSO EJBN. 2000. Detection of arbuscular mycorrhizal fungi in roots of coffee plants and crotalaria cultivated between rows. Pesqui Agropecu Bras 35(10): 2033-2042.

DA SILVA RF, DE MARCO R, BERTOLLO GM, MATSOUKA M AND MENEGOL DR. 2015. Influência do uso do solo na ocorrência e diversidade de FMAs em Latossolo no Sul do Brasil. Semin Agrar 36(3): 1851-1862.

DJEKOUNE AO, MESSAOUDI K AND AMARA K. 2017. Incremental circle hough transform: An improved method for circle detection. Opt - Int J Light Electron Opt 133: 17-31.

DUDA RO AND HART PE. 1972. Use of the Hough Transformation to Detect Lines and Curves in Pictures. Commun ACM 15(1): 11-15.

FANG CY, FUH CS, YEN PS, CHERNG S AND CHEN SW. 2004. An automatic road sign recognition system based on a computational model of human recognition processing. Comput Vis Image Underst 96: 237-268.

FERREIRA MS AND GALO MLBT. 2013. *Chlorophyll a* spatial inference using artificial neural network from multispectral images and *in situ* measurements. An Acad Bras Cienc 85: 519-532.

FREEMAN JA AND SKAPURA DM.1991. Neural Networks: Algorithms, Applications and Programming Techniques, MA: Addison-Wesley, Reading, 550 p.

GERDEMANN JW AND NICOLSON TH. 1963. Spores of micorrhizal endogone species extract tend for soil by wet sieving and decating. Trans Br Mycol Soc 46 (2): 235-244.

GIANINAZZI-PEARSON V. 1996. Plant Cell Responses to Arbuscular Mycorrhizal Fungi: Getting to the Roots of the Symbiosis. The Plant Cell 8(10): 1871-1883.

GONZALEZ RC AND WOODS RE. 2010. Digital Image Processing, 3rd ed., São Paulo: Peason Prentice Hall, 976 p.

GOTO BT AND MAIA LC. 2006. Glomerospores: a new denomination for the spores of Glomeromycota, a group molecularly distinct from the Zygomycota. Mycotaxon 96: 129-132.

GROOVER MP. 2007. Automation, Production Systems, and Computer-Integrated Manufacturing 3rd ed., Upper Saddle River, NJ, USA: Prentice Hall Press, 840 p.

HAYKIN SS. 1999. Neural Networks: A Comprehensive Foundation, 2nd ed., Prentice Hall, 842 p.

INVAM - INTERNATIONAL CULTURE COLLECTION OF (VESICULAR) ARBUSCULAR MYCORRHIZAL FUNGI. 2015. Morgantown: West Virginia Agriculture and Forestry Experimental Station. Available at: http://invam.wvu.edu/ [Accessed October 13, 2015].

KOTHARI S, CHAUDRY Q AND WANG MD. 2009. Automated cell counting and cluster segmentation using concavity detection and ellipse fitting techniques. In Proc. IEEE Int. Symp. Biomedical Imaging: From Nano to Macro. Boston, MA, IEEE: 795-798.

LANDIS JR AND KOCH GG. 1977. The measurement of observer agreement for categorical data. Biometrics 33: 159-174.

LONGO S, NOUHRA E, GOTO BT, BERBARA RL AND URCELAY C. 2014. Effects of fire on arbuscular mycorrhizal fungi in the Mountain Chaco Forest. For Ecol Manage 315: 86-94.

MELO CAO, LOPES JG, ANDRADE AO, TRINDADE RMP AND MAGALHÃES RS. 2017. Semi-Automated Counting of Arbuscular Mycorrhizal Fungi Spores Using Artificial Neural Network. IEEE Latin America Transactions 15(8): 1566-1573.

MELO GJA, GOMES V, BACCILI CC, ALMEIDA LAL AND LIMA ACC. 2015. A robust segmentation method for counting bovine milk somatic cells in microscope slide images. Comput Electron Agric 115: 142-149.

MOREIRA BC, MENDES FC, MENDES IR, PAULA TA, PRATES JUNIOR P, SALOMÃO LCC, STÜRMER SL, OTONI WC, GUARÇONI MA AND KASUYA MCM. 2015. The interaction between arbuscular mycorrhizal fungi and Piriformospora indica improves the growth and nutrient uptake in micropropagation-derived pineapple plantlets. Sci Hortic (Amsterdam) 197: 183-192.

MOREIRA FMS AND SIQUEIRA JO. 2006. Microbiologia E Bioquimica Do Solo, 2nd ed., Editora UFLA, 744 p.

MORTON JB. 1988. Taxonomy of VA mycorrhizal fungi: classification, nomenclature and identification. Mycotaxon 32: 267-324.

NAZLIBILEK S, KARACOR D, ERCAN T, SAZLI MH, KALENDER O AND EGE Y. 2014. Automatic segmentation, counting, size determination and classification of white blood cells. Measurement 55: 58-65.

POOMCOKRAK J AND NEATPISARNVANIT C. 2008. Red blood cells extraction and counting. The 3rd Int Symp Biom Engin Proc. Int. Symp. Biomedical Eng: 199-203.

SCHENCK NC AND PEREZ Y. 1990. Manual for identification of VA mycorrhizal fungi, 3rd ed., Synerg. Publ. Gainesville, Florida, 286 p.

SCHÜßLER A, MOLLENHAUER D, SCHNEPF E AND KLUGE M. 1994. Geosiphon pyriforme, an Endosymbiotic Association of Fungus and Cyanobacteria: the Spore Structure Resembles that of Arbuscular Mycorrhizal (AM) Fungi. Bot Acta 107: 36-45.

SIEVERDING E. 1991. Vesicular-arbuscular Mycorrhiza Management in Tropical Agrosystems. GTZ, 371 p.

SIQUEIRA J, SAGGIN-JÚNIOR O, FLORES-AYLAS W AND GUIMARÃES PTG. 1998. Arbuscular mycorrhizal inoculation and superphosphate application influence plant development and yield of coffee in Brazil. Mycorrhiza 7(6): 293-300.

SMITH EE AND READ JD. 1997. Mycorrhizal symbiosis, 2nd ed., San Diego: Academic Press, 605 p.

SOUCHIE EL, AZCÓN R, BAREA JM, SILVA EMR AND SAGGIN-JÚNIOR OJ. 2010. Enhancement of clover growth by inoculation of P-solubilizing fungi and arbuscular mycorrhizal fungi. An Acad Bras Cienc 82: 771-777.

SU MC, CHENG CY AND WANG PC. 2014. A neural-network-based approach to white blood cell classification. Sci World J 2014.

TAN K, CHAI Y, SONG W AND CAO X. 2014. Identification of diseases for soybean seeds by computer vision applying BP neural network. Int J Agric Biol Eng 7(3): 43-50.

TRAUTH MH. 2006. MATLAB® Recipes for Earth Sciences 1st ed., Potsdam-Germany: Springer, 240 p.

TSUJI S AND MATSUMOTO F. 1978. On Detection of Ellipses by a Modified Hough Transformation. IEEE Trans Comput C-27(8): 777-781.

TULLIO M, CALVIELLO F AND REA E. 2012. Effect of Compost Based Substrate and Mycorrhizal Inoculum in Potted Geranium Plants. J Life Sci 6: 771-775.

WALKER C AND VESTBERG M. 1998. Synonymy Amongst the Arbuscular Mycorrhizal Fungi: *Glomus claroideum, G. maculosum, G. multisubstenum* and *G. fistulosum*. Ann Bot 82(5): 601-624.

YAO Z AND YI W. 2016. Curvature aided Hough transform for circle detection. Expert Syst Appl 51: 26-33.

ZHAOYONG Z, YU L, DONG S, HAIHUI Z, DONGJIAN H AND YANG C. 2016. Detection of moldy core in apples and its symptom types using transmittance spectroscopy. Int J Agric and Biol Eng 9(6): 148-155.